The COOH-Terminal Peptide of Platelet Factor-4 Variant (CXCL4L1/PF-4var[47-70]) Strongly Inhibits Angiogenesis and Suppresses B16 Melanoma Growth *In vivo*

Jo Vandercappellen[1], Sandra Liekens[2], Annelies Bronckaers[2], Samuel Noppen[1], Isabelle Ronsse[1], Chris Dillen[1], Mirella Belleri[3], Stefania Mitola[3], Paul Proost[1], Marco Presta[3], Sofie Struyf[1], and Jo Van Damme[1]

Abstract

Chemokines influence tumor growth directly or indirectly via both angiogenesis and tumor-leukocyte interactions. Platelet factor-4 (CXCL4/PF-4), which is released from α-granules of activated platelets, is the first described angiostatic chemokine. Recently, it was found that the variant of CXCL4/PF-4 (CXCL4L1/PF-4var) could exert a more pronounced angiostatic and antitumoral effect than CXCL4/PF-4. However, the molecular mechanisms of the angiostatic activities of the PF-4 forms remain partially elusive. Here, we studied the biological properties of the chemically synthesized COOH-terminal peptides of CXCL4/PF-4 (CXCL4/PF-4[47-70]) and CXCL4L1/PF-4var (CXCL4L1/PF-4var[47-70]). Both PF-4 peptides lacked monocyte and lymphocyte chemotactic activity but equally well inhibited (25 nmol/L) endothelial cell motility and proliferation in the presence of a single stimulus (i.e., exogenous recombinant fibroblast growth factor-2). In contrast, when assayed in more complex angiogenesis test systems characterized by the presence of multiple mediators, including *in vitro* wound-healing (2.5 nmol/L versus 12.5 nmol/L), Matrigel (60 nmol/L versus 300 nmol/L), and chorioallantoic membrane assays, CXCL4L1/PF-4var[47-70] was found to be significantly (5-fold) more angiostatic than CXCL4/PF-4[47-70]. In addition, low (7 μg total) doses of intratumoral CXCL4L1/PF-4var[47-70] inhibited B16 melanoma growth in mice more extensively than CXCL4/PF-4[47-70]. This antitumoral activity was predominantly mediated through inhibition of angiogenesis (without affecting blood vessel stability) and induction of apoptosis, as evidenced by immunohistochemical and fluorescent staining of B16 tumor tissue. In conclusion, CXCL4L1/PF-4var[47-70] is a potent antitumoral and antiangiogenic peptide. These results may represent the basis for the design of CXCL4L1/PF-4var COOH-terminal–derived peptidomimetic anticancer drugs. *Mol Cancer Res; 8(3); 322–34.* ©2010 AACR.

Introduction

Platelet factor-4 (CXCL4/PF-4) has been identified as a tetrameric heparin-binding protein released from the α-granules of activated platelets long before the term chemokine was introduced (1). Later, small chemotactic cytokines, which are essential mediators in leukocyte migration to inflammatory sites and to secondary lymphoid organs, were identified and named chemokines (2). However, chemokines have additional biological functions, influencing angiogenesis and tumor development (3, 4). They are classified into four groups depending on the positioning of the conserved cysteines in the NH2-terminal part—CXC, CC, CX3C, and C chemokine ligands (5)—and they generally bind to G protein–coupled seven-transmembrane receptors (GPCR) designated CXCR or CCR (6, 7). The well-characterized interleukin-8 (CXCL8/IL-8) is classified among the ELR+ CXC chemokines (presence of the tripeptide glutamic acid–leucine–arginine preceding the CXC motif), which bind to CXCR2 and chemoattract neutrophilic granulocytes and exert angiogenic activity (8, 9). In contrast, CXCL4/PF-4 belongs to the ELR− CXC chemokine group and is angiostatic (10). Besides its angiostatic activity, CXCL4/PF-4 is implicated in different biological processes, such as coagulation, promotion of neutrophil cell adhesion to endothelium, and inhibition of megakaryopoiesis and hematopoiesis (11-13). Although CXCL4/PF-4 was the first discovered chemokine, the mechanisms by which it exerts its pleiotropic biological activities are complex and remain partially elusive. The proposed receptor for CXCL4/PF-4, named CXCR3-B (14), might

Authors' Affiliations: [1]Laboratory of Molecular Immunology and [2]Laboratory of Virology and Chemotherapy, Rega Institute for Medical Research, University of Leuven, Leuven, Belgium and [3]Unit of General Pathology and Immunology, Department of Biomedical Sciences and Biotechnology, School of Medicine, University of Brescia, Brescia, Italy

Note: S. Struyf and J. Van Damme contributed equally to this work.

Corresponding Author: Jo Van Damme, Laboratory of Molecular Immunology, Rega Institute, University of Leuven, Minderbroedersstraat 10, B-3000 Leuven, Belgium. Phone: 32-16337348; Fax: 32-16337340. E-mail: jo.vandamme@rega.kuleuven.be

doi: 10.1158/1541-7786.MCR-09-0176

©2010 American Association for Cancer Research.

not mediate all its effects. The variant of CXCL4/PF-4, encoded by a second nonallelic gene and differing in only three amino acids, is named CXCL4L1/PF-4var (15, 16) and was isolated from thrombin-stimulated platelets (17). In a previous study, we showed that CXCL4L1/PF-4var is also produced by osteosarcoma cells (18). CXCL4L1/PF-4var was found to be a more potent angiostatic and antitumoral chemokine than CXCL4/PF-4 in different *in vitro* assays and *in vivo* models (17, 19). Previous reports have shown that shorter COOH-terminal fragments of CXCL4/PF-4 retain their angiostatic properties (20, 21). However, because the mode of action of both PF-4 forms is not fully understood, we designed COOH-terminal peptides of CXCL4/PF-4 and CXCL4L1/PF-4var, named CXCL4/PF-4[47-70] and CXCL4L1/PF-4var[47-70]. We found that both peptides lack monocyte and lymphocyte chemotactic response but retain their angiostatic activity. In addition, we showed that similar to the intact PF-4 forms, CXCL4L1/PF-4var[47-70] is a more potent angiostatic and antitumoral peptide than CXCL4/PF-4[47-70] in different *in vitro* assays and *in vivo* models. Finally, we provide evidence that the antitumoral effect of CXCL4L1/PF-4var[47-70] is predominantly mediated through inhibition of angiogenesis and induction of apoptosis.

Materials and Methods

Peptide Synthesis
The human COOH-terminal CXCL4/PF-4 peptide (CXCL4/PF-4[47-70]: NGRKICLDLQAPLYKKIIKKLLES) and CXCL4L1/PF-4var peptide (CXCL4L1/PF-4var[47-70]: NGRKICLDLQALLYKKIIKEHLES) were prepared by solid-phase peptide synthesis using fluorenyl-methoxy-carbonyl (Fmoc)–protected amino groups as previously described (22). Purification was done by reversed-phase high-performance liquid chromatography (RP-HPLC) using a Source 5RPC column (GE Healthcare). Proteins were eluted from the column in an acetonitrile gradient in 0.1% trifluoroacetic acid, and UV absorption was monitored at 220 nm. The molecular mass and the sequence of the peptides were confirmed by Esquire LC electrospray ion trap mass spectrometry (MS; Bruker) and 491 Procise cLC protein sequence analysis (Applied Biosystems). The extracted ion chromatogram (theoretical values of m/z for +2 to +6 ions: 1,413.7, 942.8, 707.4, 566.1, and 471.9) shows the relative amount of CXCL4L1/PF-4var[47-70] with an average M_r of 2,826. Lyophilized peptides were dissolved in sterile PBS (Lonza BioWhittaker, Cambrex Bio Science), stabilized in 0.02% (w/v) human serum albumin (HSA; Belgian Red Cross), supplemented with 0.01% (v/v) Tween 20 (Sigma-Aldrich), and stored at –20°C before use. Control buffer used in all experiments was prepared the same way as the peptides [i.e., by lyophilization of the same HPLC solvent (25% acetonitrile/0.1% trifluoroacetic acid) and reconstitution in PBS].

SDS-PAGE
The purity and molecular mass of both COOH-terminal peptides were examined by SDS-PAGE (23). Different amounts (30 and 10 ng/lane) of both peptides were loaded on a Tris/tricine gel. The stacking, spacer, and separating gels contained 5% total concentration of acrylamide and bisacrylamide monomers in w/v percent (T) and 5% amount of bisacrylamide cross-linker relative to T in w/w percent (C), 10% T and 3.3% C, and 13% T and 5% C, respectively. Molecular mass markers (Bio-Rad Laboratories) were lysozyme and aprotinin (relative molecular weights of 14.4 and 6.5 kDa, respectively). Peptides were visualized by silver staining.

Cell Cultures
Human activated T cells were obtained from peripheral blood mononuclear cells, purified from buffy coats of healthy donors provided by the Blood Transfusion Center of Leuven (Leuven, Belgium) as previously described (23). These peripheral blood mononuclear cells were stimulated with 2 μg/mL phytohemagglutinin (Sigma-Aldrich) for 3 d in RPMI 1640 supplemented with 10% (v/v) FCS (PAA Laboratories). Activated lymphocytes were cultured at 2×10^6 cells/mL for 2 to 3 wk in the presence of 50 units/mL IL-2 (PeproTech) before use in chemotaxis assays. The human monocytic cell line THP-1 (TIB-202, American Type Culture Collection) was grown in suspension in RPMI 1640 supplemented with 10% (v/v) FCS.

Human dermal microvascular endothelial cells (HMVEC-d; Lonza Cambrex Bio Science) were cultured following the manufacturer's instructions in endothelial basal medium (EBM-2) supplemented with the endothelial growth medium EGM-2MV Bullet kit (Lonza Cambrex Bio Science). The fetal bovine aortic endothelial cell line (GM7373) and human umbilical vein endothelial cells (HUVEC) were cultured in DMEM plus 10% (v/v) FCS.

B16 melanoma was orthotopically propagated in C57BL/6 mice and cultured in Eagle's MEM with Earle's salts (Invitrogen) buffered with $NaHCO_3$ and supplemented with 10% (v/v) FCS and L-glutamine.

In vitro Chemotaxis
The chemotactic activities of the synthetic peptides CXCL4/PF-4[47-70] and CXCL4L1/PF-4var[47-70] were tested on activated T cells and THP-1 cells. Human synthetic CXCL11/I-TAC (22) and natural human CCL2/MCP-1, purified in our laboratory (23), were used as positive controls. Chemotaxis of activated T cells was done in HBSS supplemented with 0.1% (w/v) HSA at 2×10^6 cells/mL in the Boyden microchamber (Neuro Probe) with fibronectin-coated, polyvinylpyrrolidone-free polycarbonate membranes (5-μm pore size; Corning Separations Division) for 3 h at 37°C. Activated T cells that migrated through the membrane were stained with Hemacolor staining solutions (Merck) and counted microscopically in 10 oil immersion fields (×500 magnification). The chemotactic index (CI) was calculated as the number of cells that migrated to the test chemokine divided by the number

of cells that spontaneously migrated to the chemotaxis buffer [HBSS + 0.1% (w/v) HSA]. In addition, an alternative cell migration assay with detection based on an enzymatic reaction was used to study chemotaxis of THP-1 cells. The multiscreen plate (Millipore Corp.) is composed of a 96-well filter plate (5-μm pore size) and a 96-well receiver plate. Cell migration occurs through the 96-well filter plate in response to a chemotactic gradient. The THP-1 cell suspension (100 μL in 96-well filter plate at a concentration of 3.5×10^6 cells/mL) and test samples (150 μL in 96-well receiver plate) were diluted in RPMI 1640 without phenol red and L-glutamine (Lonza Cambrex Bio Science) supplemented with 0.1% (w/v) bovine serum albumin (BSA; endotoxin-free; Sigma-Aldrich). After 3-h incubation at 37°C, the upper 96-well filter plate was removed and the cells in the lower receiver plate were quantified using the luminescence ATP detection system (Perkin-Elmer Life and Analytical Sciences). This highly sensitive enzymatic ATPlite assay measures the production of light caused by the reaction of ATP, derived from the cells after lysis, with added luciferase and D-luciferin. The emitted light is proportional to the ATP concentration and the number of cells and was measured in a luminescence reader (FL600 microtiter plate fluorescence reader; Biotek Instruments). The CI was calculated by dividing the luminescence value of the test sample by the luminescence value of the chemotaxis buffer (control).

Endothelial Cell Migration

Inhibition of endothelial cell migration *in vitro* has previously been described in detail (18). Briefly, confluent monolayers of mitomycin C–treated HMVEC were wounded with a plastic pipette tip and repair was monitored microscopically after a 24-h treatment with natural human CXCL4/PF-4, recombinant human CXCL4L1/PF-4var, synthetic CXCL4/PF-4[47-70], or CXCL4L1/PF-4var[47-70] in culture medium [i.e., EBM-2 medium supplemented with the EGM-2MV Bullet kit containing FCS, ascorbic acid, hydrocortisone, fibroblast growth factor (FGF), vascular endothelial growth factor (VEGF), insulin-like growth factor I, and epidermal growth factor]. The difference of the width of the individual wounds before and after treatment was scored under a microscope and set at zero for control cultures. A scar, which was broader compared with the control scars (inhibition of HMVEC migration), received an inhibition score.

Time-Lapse Cell Motility Assay

Cell motility was assessed by time-lapse videomicroscopy. HUVECs were seeded at 150 cells/mm^2 in 24-well plates for 2 h and then stimulated with 30 ng/mL FGF-2 in DMEM plus 0.5% FCS in the presence or absence of increasing concentrations of CXCL4/PF-4[47-70] or CXCL4L1/PF-4var[47-70]. Constant temperature (37°C) and CO$_2$ concentration (5%) were maintained throughout the experimental period by means of a heatable stage and climate chamber. Cells were observed under an inverted microscope (Zeiss Axiovert 200M), and phase-contrast snap photographs (one frame every 15 min) were digitally recorded for 180 min. Cell paths (15-20 cells per experimental point) were generated from centroid positions, and migration parameters were analyzed with the "Migration and Chemotaxis" tool of ImageJ software.[4]

Endothelial Cell Proliferation

The cell proliferation assay was done on fetal bovine aortic endothelial GM7373 cells as described (24). Briefly, subconfluent cell cultures were incubated in DMEM containing 0.4% FCS plus 10 ng/mL FGF-2 in the presence or absence of increasing concentrations of CXCL4/PF-4[47-70] or CXCL4L1/PF-4var[47-70]. After 24 h, cells were trypsinized and counted in a Bürker chamber. Data (mean ± SD of two independent experiments in triplicate) were expressed as percentage of cell proliferation induced by FGF-2.

Matrigel Assay

Wells of a 48-well plate (Falcon, BD Biosciences) were coated with Matrigel (one half diluted in HMVEC culture medium, final concentration of 10.55 mg/mL; BD Matrigel basement membrane matrix, high growth factor concentration, phenol red–free) and allowed to solidify for 30 min at 37°C. Subsequently, 55,000 HMVECs in 400 μL of EBM-2 with EGM-2MV Bullet kit were seeded in each well and incubated with peptide at 37°C. Each peptide was tested at different concentrations in triplicate. In at least three control wells per test plate, tube formation was allowed in pure culture medium (i.e., in the absence of inhibitory peptide). Tube formation was monitored every hour with transmitted light by using an Axiovert 200 M inverted microscope, equipped with an EC Plan-Neofluar 10×/0.30 dry objective and a XL-3 incubator. Pictures were taken with an AxioCam MRm camera and processed with AxioVision software release 4.6.3 (Zeiss). For each experiment, the time point chosen for evaluation was the minimal incubation period necessary for optimal tube formation under our experimental conditions (11-15 h after seeding). The total length of the tubular structures formed in each well was calculated in 25 microscopic fields. The results are expressed as the mean percentage inhibition of tube formation compared with the control.

CAM Assay

Fresh fertilized chicken eggs (*Gallus gallus*) were incubated for 3 d at 37.6°C. On day 3, albumin (3-4 mL) was removed to detach the egg shell from the developing chorioallantoic membrane (CAM) and a window was opened in the shell exposing the CAM. The window was covered with cellophane tape, and the eggs were further incubated. On day 9, the peptides were applied on sterile plastic discs (8-mm diameter), which were allowed to dry under sterile conditions. A solution of cortisone acetate (100 μg/disc; Certa) was added to all discs to prevent an inflammatory

---

[4] http://rsbweb.nih.gov/ij

response. A dried control disc loaded with dilution buffer was placed on the CAM ~1 cm away from the disc containing the peptide. Next, the windows were covered, and the eggs were incubated for 2 more days. On day 11, the eggs were opened, the CAM was removed, and angiogenesis was assessed. Pictures of each CAM were taken under a stereomicroscope (7.5×, Moticam 2300) using a digital camera (Motic Mc camera 2.1). All vessels intersecting two concentric circles positioned in the treated area were counted double blind and independently by two investigators. Results are represented as the mean percentage inhibition of the number of blood vessels intersecting the test disc compared with the control disc.

In addition, peptides were tested for their ability to inhibit FGF-2–induced angiogenesis in the gelatin sponge CAM assay. Therefore, at day 9 of embryonic development, 2 mm³ sterilized gelatin sponges (Gelfoam, Upjohn) containing 5 μg peptide (CXCL4/PF-4[47-70] or CXCL4L1/PF-4var[47-70]) with or without 500 ng FGF-2 (Sigma-Aldrich) were placed on top of the CAM. After 48 h, CAMs were fixed *in ovo* with 4% paraformaldehyde in PBS for 1 h, dehydrated in graded ethanol, embedded in paraffin, and serially sectioned at 7 μm according to a plane parallel to their surface. Next, sections were stained with H&E. To determine the number of blood vessels, pictures of the CAM tissue around the gelatin sponge were taken at a ×100 magnification (Zeiss Imager Z.1 microscope). Results are expressed as the mean number of blood vessels (counted double blind by two independent investigators) ± SEM.

Tumor Model

Experiments were conducted with 6- to 8-wk-old female athymic *nu/nu* mice (NMRI background, Elevage Janvier) kept in a specific pathogen-free environment (three independent experiments). B16 melanoma cells in log phase (2 × 10⁶ resuspended in 200 μL PBS) were injected s.c. on day 0 in the right dorsal flank. Animals were treated intratumorally with control, 1 μg CXCL4/PF-4[47-70], or 1 μg CXCL4L1/PF-4var[47-70] three times a week starting from day 1 (total dose equals 7 μg peptide/mouse). The external tumor volume was measured with calipers thrice a week and calculated using the following formula: $(4\pi a b^2)/3$ (*a* and *b* are the largest and smallest radius, respectively). On day 17, mice were sacrificed and tumors were resected. The exact tumor volume, based on three measured radii (*a*, *b*, and *c*), was calculated by the following formula: $(4\pi a b c)/3$. The resected tumor weight was also determined. Animal experiments were approved by the local animal ethic committee (University of Leuven, Leuven, Belgium) and conducted in conformity with the Belgian and European guidelines for the protection of animals used for scientific purposes.

Tumor Tissue Analysis for Endothelial Cells, Pericytes, and Apoptosis

For immunohistochemical analysis of B16 tumor vasculature (two independent experiments), tumors were harvested and snap frozen in liquid N_2, and sections were analyzed for the presence of blood vessels reacting with rat anti-mouse CD31 antibody (BD Biosciences) using the anti-rat immunoglobulin horseradish peroxidase detection kit from Pharmingen (BD Biosciences) followed by a counterstain with Harris' hematoxylin. Transmitted light microscopy of the whole tumor sections was done on an Axiovert 200 M with an EC Plan-Neofluar 10×/0.30 dry objective. Pictures were taken with an AxioCam MRc5 camera (2584 × 1936 color) and processed with Axio-Vision software release 4.6.3. The number of small (area <145.8 μm²), medium-size (area between 145.8 and 2,916 μm²), and large (area >2,916 μm²) blood vessels was counted semiautomatically with the AutoMeasure Plus module, double blind, and independently by two investigators. In addition, vessel stabilization was analyzed by staining of pericytes. Frozen sections were blocked in PBS containing 5% normal goat serum, 0.01% Tween 20, and 0.2% BSA. Next, sections were incubated with rat monoclonal anti-CD31 antibody (1:400) and mouse monoclonal α-smooth muscle actin antibody (1:250; Sigma-Aldrich) in PBS supplemented with 0.2% BSA. After overnight incubation at 4°C, sections were washed with PBS/0.01% Tween 20/0.1% BSA and incubated overnight at 4°C with Alexa Fluor 350–conjugated goat anti-rat IgG (1:450 diluted in PBS with 0.2% BSA; Molecular Probes, Invitrogen) and Alexa Fluor 647–conjugated donkey anti-mouse IgG (1:1,500; Molecular Probes). Finally, slides were washed and mounted.

For the detection of apoptotic cells in tumor tissue, we used the terminal deoxynucleotidyl transferase–mediated dUTP nick end labeling (TUNEL) assay with the ApoAlert DNA fragmentation kit (Clontech). Cell nuclei were stained with 1.1 μmol/L 4′,6-diamidino-2-phenylindole (DAPI; Sigma-Aldrich). Fluorescence microscopy was done with an Axiovert 200 M equipped with a Lambda DG-4 light source (Sutter Instrument Co.), DAPI and fluorescein filter sets, an EC Plan-Neofluar 10×/0.30 dry objective, and an AxioCam MRm camera (1292 × 968 mono). The whole tumor section was automatically analyzed for apoptosis. Data are expressed as a percentage of the apoptotic surface area (green) compared with the total surface area (blue).

Statistical Analysis

All data were analyzed using Statistica software (StatSoft, Inc.). All results were evaluated by the Mann-Whitney U test (*, $P < 0.05$; **, $P < 0.01$; ***, $P < 0.001$).

Results

Preparation of COOH-Terminal Peptides of CXCL4/PF-4 and CXCL4L1/PF-4var

COOH-terminal peptides of human CXCL4/PF-4 and CXCL4L1/PF-4var, abbreviated CXCL4/PF-4[47-70] and CXCL4L1/PF-4var[47-70], were prepared by solid-phase peptide synthesis using Fmoc-protected amino groups (22). Final purification was done by RP-HPLC using a

Source 5RPC column. CXCL4L1/PF-4var$^{47-70}$ was eluted between 24% and 26% acetonitrile. Part of the column effluent was split to an electrospray ion trap mass spectrometer to determine the average molecular mass (M_r). The averaged MS spectra of CXCL4L1/PF-4var$^{47-70}$ shown in Fig. 1 indicate the charges of the detected ions (+3 to +5) and the deconvoluted spectrum that was calculated from these charged ions. MS, in combination with NH$_2$-terminal amino acid sequencing, confirmed the purity and the exact sequence of both CXCL4/PF-4$^{47-70}$ and CXCL4L1/PF-4var$^{47-70}$. In addition, the purity and the molecular mass of both peptides were confirmed by SDS-PAGE.

The COOH-Terminal Peptides of Human CXCL4/PF-4 and CXCL4L1/PF-4var Are Poor Chemoattractants but Potent Angiostatic Factors *In vitro*

CXC chemokines are potent chemoattractants for either neutrophils (e.g., CXCL8/IL-8) or activated T lymphocytes (e.g., CXCL10/IP-10). We have previously shown that both CXCL4/PF-4 and CXCL4L1/PF-4var are unable to stimulate phagocyte migration *in vitro* (18). CXCL4/PF-4$^{47-70}$ and CXCL4L1/PF-4var$^{47-70}$ were now tested for their potential to chemoattract activated T cells in the microchamber chemotaxis assay. It was found that CXCL4/PF-4$^{47-70}$ and CXCL4L1/PF-4var$^{47-70}$ are not chemotactic at all on activated T cells. In contrast, the CXCR3 ligand CXCL11/I-TAC was still attracting T cells at 10 nmol/L (Fig. 2A). Next, it was verified whether CXCL4/PF-4$^{47-70}$ and CXCL4L1/PF-4var$^{47-70}$ induce chemotaxis of monocytic THP-1 cells in the Millipore system. CXCL4/PF-4$^{47-70}$ and CXCL4L1/PF-4var$^{47-70}$ were not chemotactic for THP-1 cells, whereas the CC chemokine CCL2/MCP-1 was very effective on monocytic cells, as a CI of 7 was observed at only 0.3 nmol/L (Fig. 2B).

We also verified whether endothelial cell migration and motility, important prerequisites for angiogenesis, were inhibited by CXCL4/PF-4$^{47-70}$ and CXCL4L1/PF-4var$^{47-70}$. First, it was shown that, in sharp contrast to the lack of monocyte and lymphocyte chemotactic activity, both peptides inhibited endothelial cell migration following the mechanical wounding of a HMVEC monolayer in the presence of multiple growth factors (Fig. 2C). Interestingly, CXCL4L1/PF-4var$^{47-70}$ exerted a significant effect at doses as low as 2.5 nmol/L, whereas a 5-fold higher dose was required for CXCL4/PF-4$^{47-70}$ (Fig. 2D). As a control, CXCL4/PF-4 and CXCL4L1/PF-4var were also tested in this assay. The results confirm that CXCL4L1/PF-4var inhibits endothelial cell migration at 1 nmol/L, being therefore a 20-fold more potent inhibitor than CXCL4/PF-4 (18, 19). Next, it was found that both PF-4 peptides (from 5 nmol/L onwards) significantly inhibited FGF-2–induced HUVEC motility as observed by time-lapse microscopy (Fig. 3A). In addition, the effect of CXCL4/PF-4$^{47-70}$ and CXCL4L1/PF-4var$^{47-70}$ on FGF-2–stimulated bovine aortic endothelial GM7373 cell proliferation was investigated. Both peptides inhibited FGF-2–induced GM7373 cell proliferation in a similar manner, ±40% inhibition be-

ing observed when CXCL4/PF-4$^{47-70}$ or CXCL4L1/PF-4var$^{47-70}$ was tested at 25 nmol/L (Fig. 3B).

We conclude that CXCL4/PF-4$^{47-70}$ and CXCL4L1/PF-4var$^{47-70}$ are potent angiostatic peptides rather than inflammatory mediators responsible for monocyte or lymphocyte recruitment, and depending on the test system and the experimental conditions, CXCL4L1/PF-4var$^{47-70}$ was found to be more potent than CXCL4/PF-4$^{47-70}$.

CXCL4L1/PF-4var$^{47-70}$ Is a Broad-Spectrum Angiogenesis Inhibitor *In vitro* and *In vivo*

To better evaluate their angiostatic activities, CXCL4/PF-4$^{47-70}$ and CXCL4L1/PF-4var$^{47-70}$ were further investigated in a morphogenic test on Matrigel *in vitro* and in the chick embryo CAM assay *in vivo*. HMVECs grown
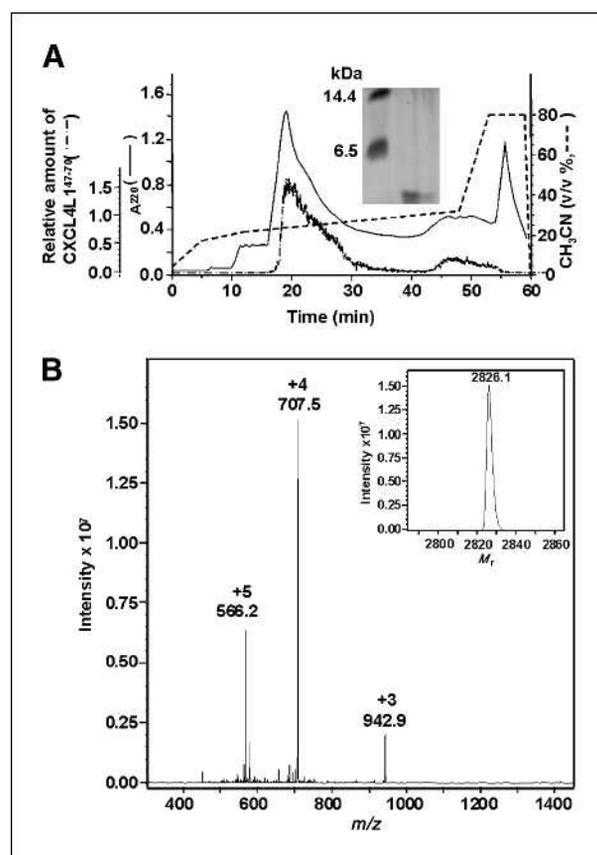

FIGURE 1. Purification of synthetic CXCL4L1/PF-4var$^{47-70}$ by RP-HPLC and MS. A, peptide was recovered from the RP-HPLC column in an acetonitrile gradient (0-80%) and UV absorbance was monitored at 220 nm (expressed as absorption units). Part of the column effluent was split to a mass spectrometer. The extracted ion chromatogram shows the relative amount of CXCL4L1/PF-4var$^{47-70}$ with an average M_r of 2,826. The purity and M_r of CXCL4L1/PF-4var$^{47-70}$ in a pool from fraction 18 to 22 (30 and 10 ng/lane) is shown on SDS-PAGE (inset). Molecular mass markers represent lysozyme (14.4 kDa) and aprotinin (6.5 kDa). B, averaged MS spectrum (m/z versus abundance) of CXCL4L1/PF-4var$^{47-70}$–containing fractions eluting between 18 and 22 min. The charge and mass of the detected ions (+ 3 to + 5) are indicated on top of the peaks and the deconvoluted spectrum is given as an inset.
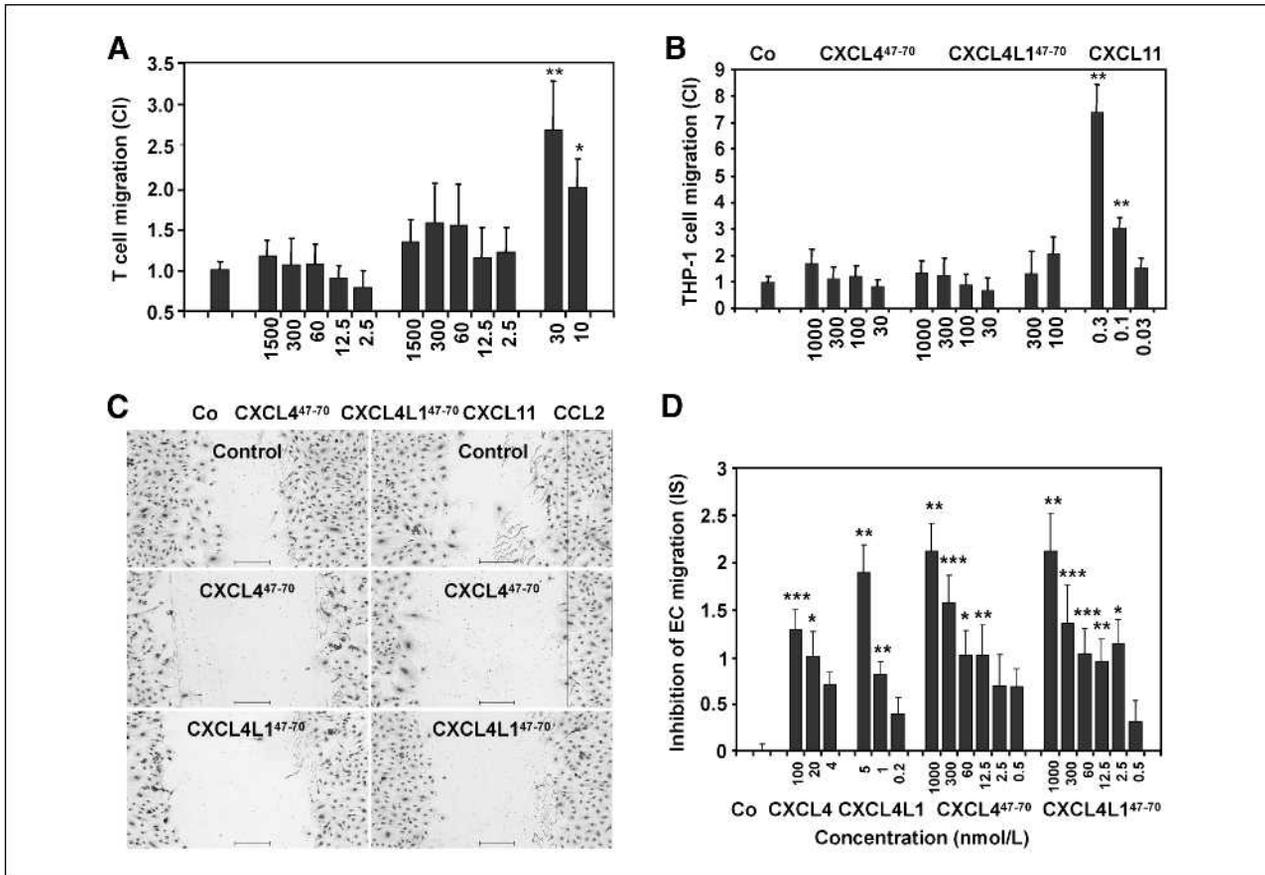
FIGURE 2. Effect of CXCL4/PF-4$^{47-70}$ and CXCL4L1/PF-4var$^{47-70}$ on the migration of activated T cells, monocytic THP-1 cells, and endothelial cells. Synthetic CXCL4/PF-4$^{47-70}$ and CXCL4L1/PF-4var$^{47-70}$ were tested for their ability to induce migration of activated T cells. A, CXCL11/I-TAC was used as positive control. B, synthetic CXCL4/PF-4$^{47-70}$, CXCL4L1/PF-4var$^{47-70}$, and CXCL11/I-TAC were tested in the THP-1 cell chemotaxis assay in parallel with CCL2/MCP-1 as a positive control. Results represent the mean CI (± SEM) of three or more independent experiments conducted in triplicate wells. HMVEC monolayers were wounded and repair was monitored after treatment with natural human CXCL4/PF-4, recombinant human CXCL4L1/PF-4var, CXCL4/PF-4$^{47-70}$, or CXCL4L1/PF-4var$^{47-70}$. C, representative microphotographs (two per condition) of inhibition of endothelial cell migration by 300 nmol/L of CXCL4/PF-4$^{47-70}$ or CXCL4L1/PF-4var$^{47-70}$ are shown. Scale bar, 200 μm. D, results represent average inhibition scores (IS) ± SEM from four or more independent experiments in duplicate. *, $P < 0.05$; **, $P < 0.01$; ***, $P < 0.001$, Mann-Whitney U test.

in vitro on Matrigel in the presence of a growth factor cocktail organize in capillary-like tubuli and form cords, which develop into a three-dimensional branching network. CXCL4/PF-4$^{47-70}$ and CXCL4L1/PF-4var$^{47-70}$ were added to the endothelial cell suspension, and after ~13 hours, a significant inhibition of tube formation was observed from 60 nmol/L of CXCL4L1/PF-4var$^{47-70}$ onwards, whereas CXCL4/PF-4$^{47-70}$ was only able to reduce the length of Matrigel networks from 300 nmol/L onwards (Fig. 4A and B). Thus, in analogy with the wound-healing assay, CXCL4L1/PF-4var$^{47-70}$ is 5-fold more potent than CXCL4/PF-4$^{47-70}$ as inhibitor of endothelial cell morphogenesis in the Matrigel assay. Further, we tested both peptides in the CAM assay, a widely used *in vivo* model for angiogenesis. Discs containing different amounts of CXCL4/PF-4$^{47-70}$, CXCL4L1/PF-4var$^{47-70}$ (25, 5, or 1 μg), or control solution were positioned onto the CAM at day 9 of incubation. CXCL4L1/PF-4var$^{47-70}$ at 25 or 5 μg reduced the spontaneous formation of blood vessels

(46.0 ± 4.0% or 30.7 ± 4.8% reduction in the number of blood vessels compared with the control; Fig. 4C and E). In contrast, CXCL4/PF-4$^{47-70}$, tested at different concentrations (25, 5, or 1 μg), was not able to inhibit the outgrowth of new capillaries (data not shown). In addition, an alternative CAM assay in which specific stimuli, *in casu* FGF-2, are incorporated in gelatin sponges was done to further compare the two peptides on growth factor–induced angiogenesis *in vivo*. The angiogenic effect of FGF-2 (500 ng) was inhibited more effectively by 5 μg of CXCL4L1/PF-4var$^{47-70}$ (75.7 ± 9.9% inhibition) compared with CXCL4/PF-4$^{47-70}$ (47.0 ± 11.5%; Fig. 4D), thus confirming that CXCL4L1/PF-4var$^{47-70}$ is a more potent angiostatic peptide.

Comparison of the Angiostatic CXCL4/PF-4$^{47-70}$ and CXCL4L1/PF-4var$^{47-70}$ COOH-Terminal Peptides for the Inhibition of B16 Melanoma Growth in Nude Mice

Because CXCL4L1/PF-4var$^{47-70}$ has stronger angiostatic properties than CXCL4/PF-4$^{47-70}$, as evidenced in

different angiogenesis assays (see above), we wanted to verify whether CXCL4L1/PF-4var[47-70] could also exert a more pronounced antitumoral activity. Therefore, nude mice were injected s.c. with 2×10^6 B16 melanoma cells and then intratumorally treated (thrice per week) with 1 μg CXCL4/PF-4[47-70], 1 μg CXCL4L1/PF-4var[47-70], or control buffer. Reduced tumor growth (determined by external measurement thrice per week) was observed in the CXCL4L1/PF-4var[47-70] group compared with the control group from day 9 onwards (Fig. 5A). On day 17, when mice were sacrificed and tumors were resected, a significantly smaller tumor volume and tumor weight was found in the CXCL4L1/PF-4var[47-70]–treated mice compared with the control mice (Fig. 5B and C). No difference in tumor development, and final tumor volume and weight (day 17) could be observed between the CXCL4/PF-4[47-70] (7 μg total dose)–treated mice and control mice. Next, it was verified whether the antitumoral activity of CXCL4L1/PF-4var[47-70] was mediated through inhibition of angiogenesis. Immunohistochemical evaluation of the intratumoral microvasculature by anti-CD31 staining showed a significantly lower number of small and medium-size intratumoral blood vessels in CXCL4L1/PF-4var[47-70]–treated mice compared with the control mice (Fig. 6A and B). There was no significant difference in the number of large blood vessels between the two groups. Again, at the dose used, no significant effect of CXCL4/PF-4[47-70] was seen on neovascularization within the tumor. In addition, vessel stabilization was evaluated by double immunofluorescent staining with anti-CD31 and anti–α-smooth muscle actin antibodies. Staining of B16 melanoma sections of control and peptide-treated mice revealed that almost all vessels were equally well stabilized by pericytes. Despite the change in number of small and medium-size blood vessels, no difference in percentage α-smooth muscle actin^{+} CD31^{+} small and medium-size vessels was observed between control, CXCL4/PF-4[47-70]–treated, and CXCL4L1/PF-4var[47-70]–treated mice. In addition, all large blood vessels of control, CXCL4/PF-4[47-70]–treated, and CXCL4L1/PF-4var[47-70]–treated mice were stabilized by pericytes (Fig. 6C and D). Further, staining of the whole tumor section for the detection of apoptotic cells was done using the TUNEL assay. Data are expressed as the percentage of the apoptotic surface area (green) compared with the total surface area of the tumor slide. The percentage of cells undergoing apoptosis was significantly higher in the CXCL4L1/PF-4var[47-70]–treated tumors (7.8 ± 2.7%), but not in the CXCL4/PF-4[47-70] group (4.2 ± 1.6%), compared with the control group (1.0 ± 0.2%; Fig. 7A and B). Taken together, these data show a clear inhibition of angiogenesis and an induction of apoptosis by CXCL4L1/PF-4var[47-70], resulting in significantly reduced tumor growth.

Discussion

Chemokines affect tumor development indirectly by influencing angiogenesis and tumor-leukocyte interactions, as well as directly by influencing tumor transformation, survival, growth, invasion, and metastasis (4, 25). The role played by chemokines is rather complex, as some chemokines may favor tumor growth and progression, whereas others may enhance antitumor immunity. In addition, chemokine receptors contribute to metastasis of tumor cells in tissue where the corresponding chemokine is expressed, like for the CXCR4-CXCL12/SDF axis (26, 27). In this study, we investigated the angiostatic and antitumoral activities of the COOH-terminal peptides of human CXCL4/PF-4 and CXCL4L1/PF-4var, designated CXCL4/PF-4[47-70] and CXCL4L1/PF-4var[47-70]. These peptides were chemically synthesized and purified by RP-HPLC, and their purity, relative mass, and the exact sequence were confirmed by SDS-PAGE, MS, and sequence analysis (Fig. 1). CXCL4L1/PF-4var differs from CXCL4/PF-4 in only three amino acids located in the COOH-terminal region (i.e., leucine instead of proline on position 58, glutamic acid versus lysine on position 66, and histidine instead of leucine on position 67).
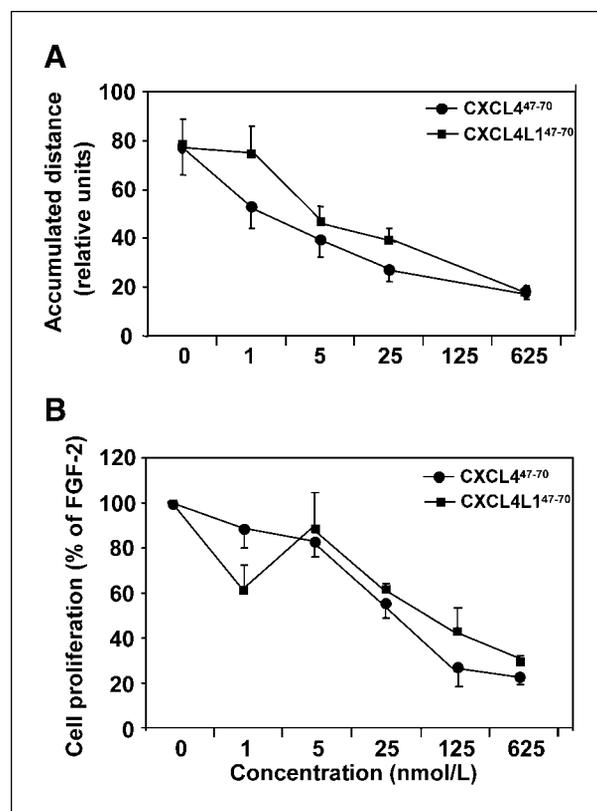

FIGURE 3. Effect of CXCL4/PF-4[47-70] and CXCL4L1/PF-4var[47-70] on FGF-2–induced endothelial cell motility and proliferation. A, different concentrations of CXCL4/PF-4[47-70] and CXCL4L1/PF-4var[47-70] were tested for their ability to inhibit FGF-2 (30 ng/mL)–induced HUVEC motility by time-lapse microscopy. Results are expressed as average accumulated distance ± SD from two independent experiments in triplicate. B, CXCL4/PF-4[47-70] and CXCL4L1/PF-4var[47-70] were tested for their ability to inhibit FGF-2 (10 ng/mL)–induced GM7373 cell proliferation. Data are expressed as mean percentage cell proliferation induced by FGF-2 ± SD from two independent experiments in triplicate.
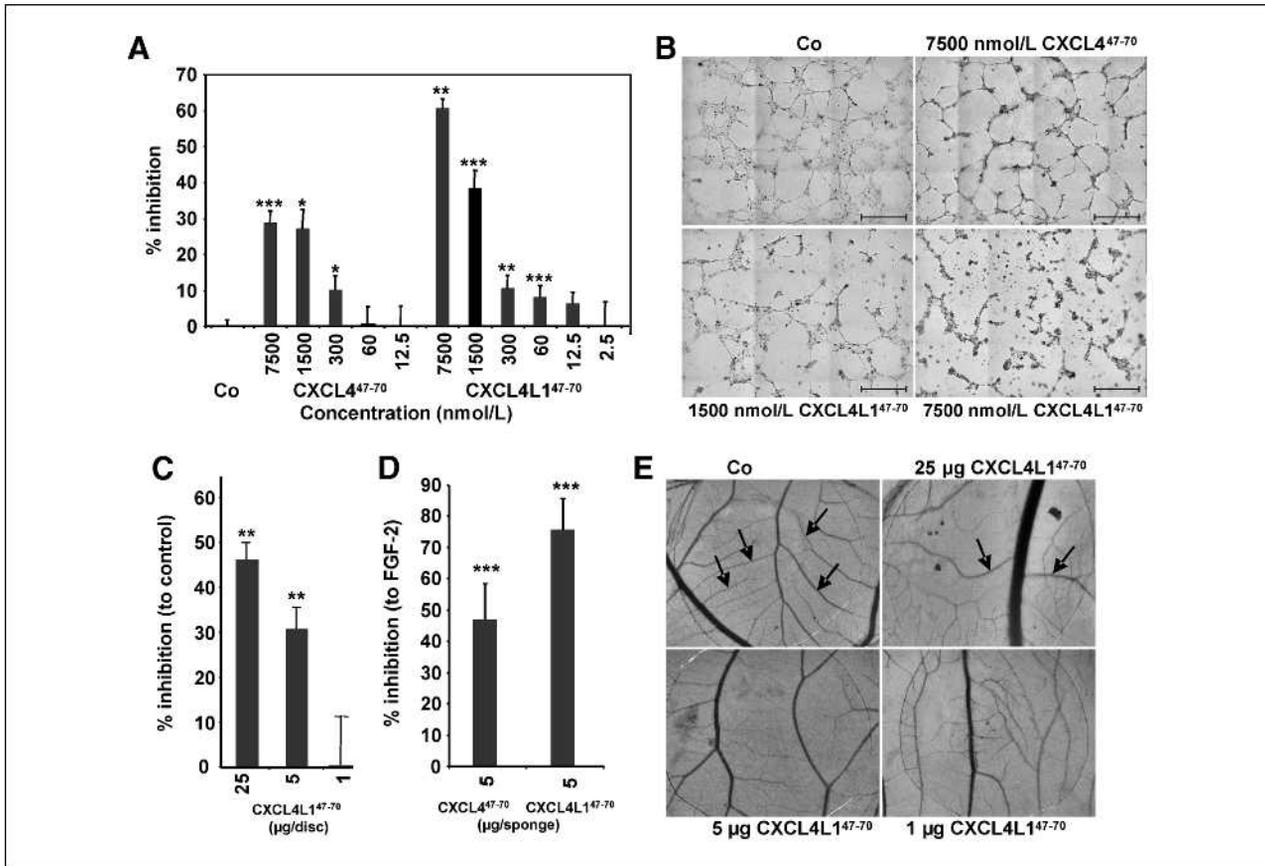
FIGURE 4. Effect of CXCL4/PF-4[47-70] and CXCL4L1/PF-4var[47-70] on endothelial cell tube formation in Matrigel and on blood vessel formation in the CAM assay. A, different concentrations of CXCL4/PF-4[47-70] and CXCL4L1/PF-4var[47-70] were tested in the Matrigel assay. Results are expressed as the mean percentage inhibition of the total length of tubes formed in peptide-treated wells compared with the total length of tubes in the buffer-treated wells ± SEM from three or more independent experiments in triplicate. *, $P < 0.05$; **, $P < 0.01$; ***, $P < 0.001$, Mann-Whitney U test. B, representative microphotographs showing inhibition of tube formation by 7,500 nmol/L CXCL4/PF-4[47-70] and 7,500 or 1,500 nmol/L CXCL4L1/PF-4var[47-70]. Scale bar, 500 μm. C, discs containing CXCL4/PF-4[47-70] or CXCL4L1/PF-4var[47-70], and control solution were applied onto the CAM. Two days later, inhibition of vascularization was evaluated. Results are represented as the mean percentage inhibition of the number of blood vessels intersecting the test disc compared with the control disc ± SEM (eight or more eggs per condition from two or more independent experiments). **, $P < 0.01$, Mann-Whitney U test. D, gelatin sponges containing 500 ng FGF-2 in combination with 5 μg CXCL4/PF-4[47-70] or CXCL4L1/PF-4var[47-70] were applied on the CAM. Results are expressed as the mean percentage inhibition of the number of blood vessels in gelatin sponges containing peptide plus FGF-2 compared with the number of blood vessels in FGF-2–containing gelatin sponges ± SEM (nine or more eggs per condition from two independent experiments). ***, $P < 0.001$, Mann-Whitney U test. E, representative photographs showing spontaneous angiogenesis on the control disc and inhibition of angiogenesis by 25 or 5 μg of CXCL4L1/PF-4var[47-70] but not by 1 μg of CXCL4L1/PF-4var[47-70]. Some blood vessels are indicated by arrows.

Because chemokines are well-known chemoattractants for phagocytes and lymphocytes (7), both COOH-terminal peptides were tested for their potential to chemoattract activated T cells and monocytic THP-1 cells. It was found that CXCL4/PF-4[47-70] and CXCL4L1/PF-4var[47-70] lack lymphocyte and monocyte chemotactic activity, whereas CXCL11/I-TAC and CCL2/MCP-1, respectively, showed a clear chemotactic response (Fig. 2A and B). In contrast, both COOH-terminal peptides markedly inhibited endothelial cell migration in the wound-healing assay containing a mixture of growth factors (Fig. 2C). CXCL4L1/PF-4var[47-70] inhibited HMVEC migration significantly at 2.5 nmol/L, whereas for CXCL4/PF-4[47-70] a 5-fold higher dose was required (Fig. 2D), indicating a stronger angiostatic activity of CXCL4L1/PF-4var[47-70] compared with

CXCL4/PF-4[47-70]. For comparison, inhibition of endothelial cell migration was obtained at 20 nmol/L CXCL4/PF-4 or 1 nmol/L CXCL4L1/PF-4var, confirming previously published data (18, 19). This allowed us to conclude that CXCL4L1/PF-4var[47-70] is equally angiostatic as the intact chemokine. In the Matrigel assay *in vitro* also containing a cocktail of growth factors, a significant inhibition of tube formation was observed from 60 nmol/L of CXCL4L1/PF-4var[47-70] onwards, whereas CXCL4/PF-4[47-70] was only able to reduce the total length of the branches of the networks from 300 nmol/L onwards (Fig. 4A). So, in analogy to the results obtained in the wound-healing assay, CXCL4L1/PF-4var[47-70] is 5-fold more potent than CXCL4/PF-4[47-70] as inhibitor of endothelial cell differentiation in the Matrigel assay. We conclude that the two

peptides behave in a different manner in different *in vitro* test systems for endothelial cell migration. In a growth factor–specific setting, both peptides inhibited FGF-2–stimulated endothelial cell motility and proliferation equally well (Fig. 3A and B). In more complex angiogenesis systems in which glycosaminoglycans (GAG), extracellular matrix proteins, a mixture of growth factors, etc. are involved, like in the *in vitro* Matrigel and wound-healing assay, CXCL4L1/PF-4var[47-70] is more potent than CXCL4/PF-4[47-70] in inhibiting angiogenesis. Further evidence for this difference in potency was found in the CAM assay *in vivo* in which 25 or 5 μg of CXCL4L1/PF-4var[47-70], but not CXCL4/PF-4[47-70], inhibited the spontaneous formation of blood vessels (46.0% or 30.7% reduction in the number of blood vessels compared with the control; Fig. 4C and E). In addition, the angiogenic effect in the presence of exogenously added FGF-2 was also inhibited more effectively by 5 μg of CXCL4L1/PF-4var[47-70] (75.7 ± 9.9% inhibition) compared with CXCL4/PF-4[47-70] (47.0 ± 11.5%) in an alternative gelatin sponge CAM assay (Fig. 4D), indicative for a significant effect of CXCL4L1/PF-4var[47-70] on endogenous mediators.

Finally, the angiostatic activities of CXCL4/PF-4[47-70] and CXCL4L1/PF-4var[47-70] were studied in the B16 melanoma model in athymic nude mice. Struyf et al. (19) already showed that intratumoral injection of intact CXCL4L1/PF-4var causes a more pronounced effect than CXCL4/PF-4 in reducing tumor size in different animal models, such as B16 melanoma, A549 adenocarcinoma, and Lewis lung carcinoma. We observed significantly reduced tumor growth in the CXCL4L1/PF-4var[47-70]–treated, but not in the CXCL4/PF-4[47-70]–treated, group (seven injections of 1 μg) from day 9 onwards. Moreover, on day 17, a significantly smaller tumor volume and weight was found in the CXCL4L1/PF-4var[47-70]–treated mice compared with the control and CXCL4/PF-4[47-70]–treated mice (Fig. 5). Because we used nude mice, an antitumoral role by infiltrating lymphocytes is excluded. CD31 staining revealed a significantly lower number of small and medium-size intratumoral blood vessels in the CXCL4L1/PF-4var[47-70]–treated mice compared with the control and CXCL4/PF-4[47-70]–treated mice (Fig. 6A and B). However, no differences in vessel stabilization by pericytes could be observed in control versus PF-4 peptide–treated mice (Fig. 6C and D). Although antiangiogenesis treatment often increases vessel stabilization, recruitment of pericytes along endothelial cells is promoted by several molecules, including platelet-derived growth factor B, sphingosine 1-phosphate, angiopoietin 1, and transforming growth factor β1 (28), and we do not expect that CXCL4L1/PF-4var[47-70] and CXCL4/PF-4[47-70] inhibit all these factors. Furthermore, the pericyte coverage index depends on the type of tumor. Treatment of B16 melanoma with a platelet-derived growth factor receptor inhibitor STI571 resulted in decreased tumor growth and vessel density without affecting the pericyte coverage (29). Thus, we confirm the findings of Hasumi et al. that monotherapy of B16 melanoma does not improve vessel stabilization.

In addition, analysis of the B16 melanoma tumor sections revealed a significantly higher percentage of cells undergoing apoptosis in the CXCL4L1/PF-4var[47-70]–treated mice (7.8%), but not in the CXCL4/PF-4[47-70] group, compared with the control group (1.0%; Fig. 7A and B). The fact that we did not observe any significant antitumoral effect for CXCL4/PF-4[47-70] in our tumor model could be due to the relatively low dose of CXCL4/PF-4[47-70] applied (seven injections of 1 μg or 0.02 mg/kg per injection) compared with previous studies (21, 30, 31). Indeed, other
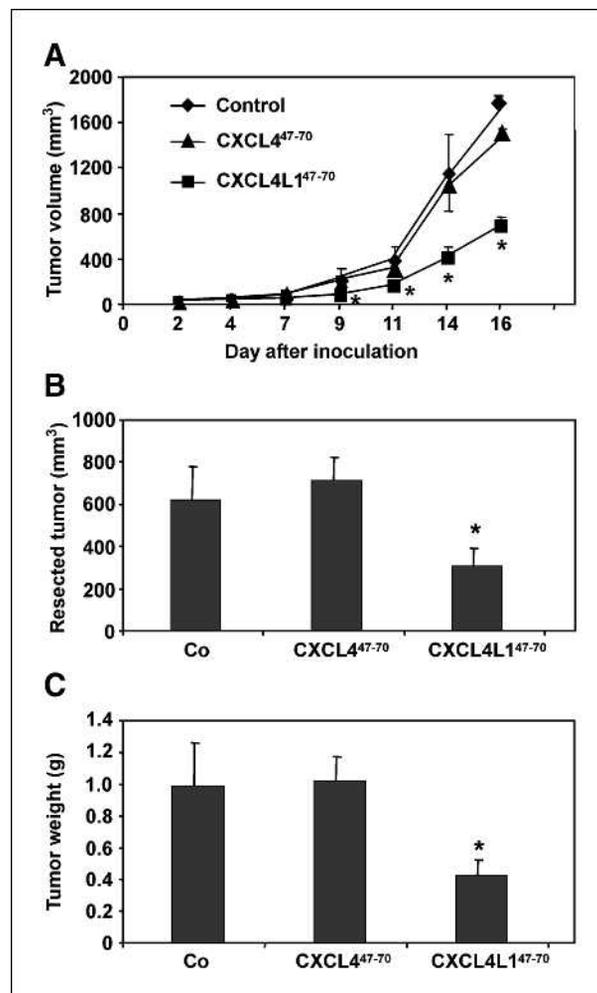

FIGURE 5. Effect of CXCL4/PF-4[47-70] and CXCL4L1/PF-4var[47-70] on B16 melanoma growth *in vivo*. Mice (*nu/nu*, three independent experiments) were injected s.c. with 2 × 10⁶ B16 melanoma cells and received intratumorally vehicle (*n* = 19 mice), 1 μg CXCL4/PF-4[47-70] (*n* = 18 mice), or 1 μg CXCL4L1/PF-4var[47-70] (*n* = 18 mice) per injection thrice a week from day 1. A, evolution of the average tumor volume (mean ± SEM) per group [formula: $(4\pi ab^2)/3$ (*a* and *b*, largest and smallest radius, respectively)]. On day 17, tumors were resected, and (B) the tumor volume (mean ± SEM) was determined [$(4\pi abc)/3$ (*a*, *b*, and *c* represent measured radii)] and the (C) resected tumor weight (mean ± SEM) was measured. Statistical analysis (Mann-Whitney *U* test) indicated a significant difference (*, $P < 0.05$) between the control mice and mice treated with CXCL4L1/PF-4var[47-70].
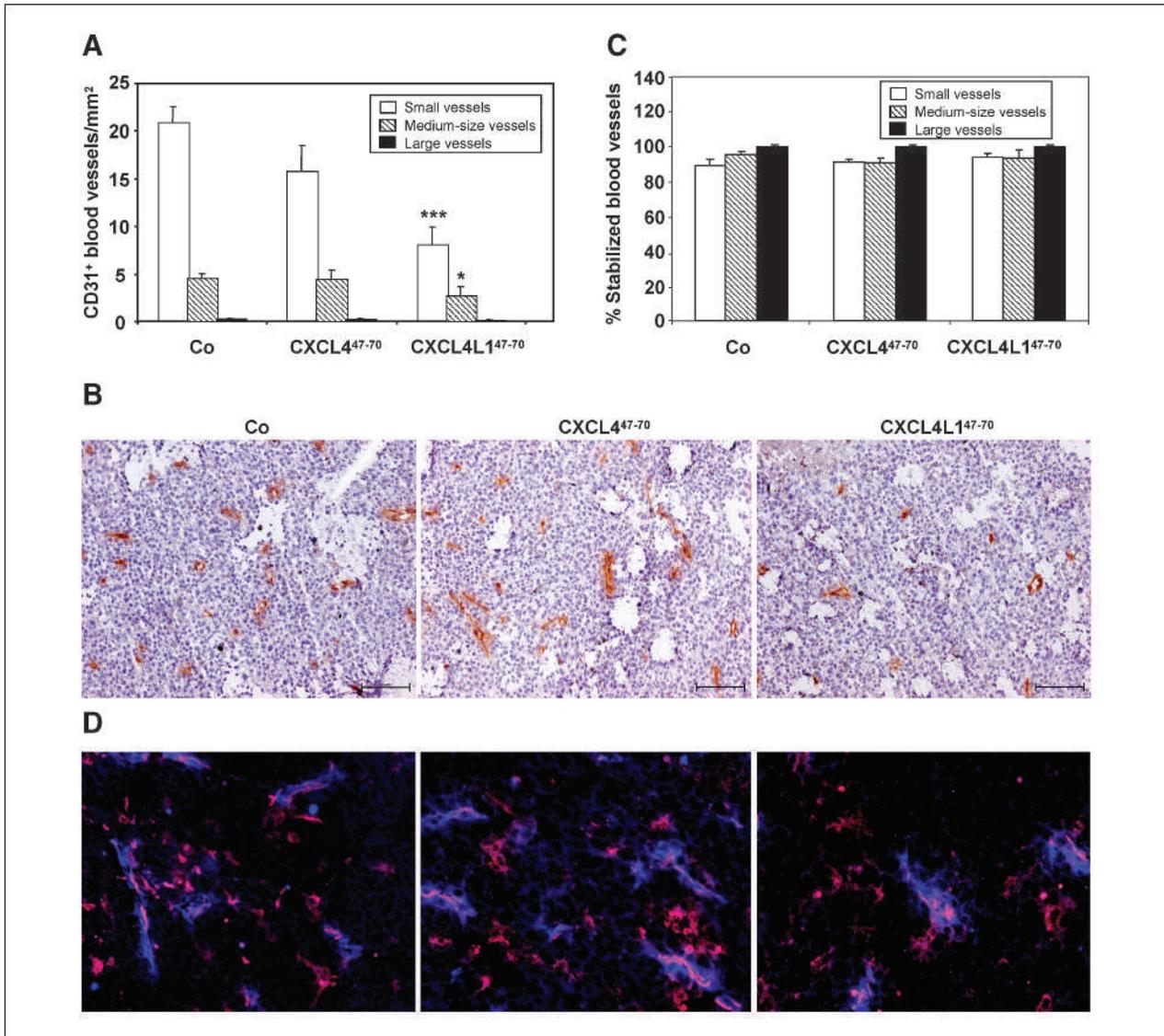
FIGURE 6. Tissue analysis of CXCL4/PF-4[47-70]–treated and CXCL4L1/PF-4var[47-70]–treated B16 melanoma for angiogenesis and vessel stabilization. Tissue sections from B16 tumors treated with control solution, 1 µg CXCL4/PF-4[47-70], or 1 µg CXCL4L1/PF-4var[47-70] per injection were evaluated for angiogenesis and vessel stabilization. A, number (mean ± SEM) of small (area <145.8 µm^2), medium-size (area between 145.8 and 2,916 µm^2), and large (area >2,916 µm^2) CD31$^+$ blood vessels per mm^2 in the peptide-treated mice compared with the control group. *, $P < 0.05$; ***, $P < 0.001$, Mann-Whitney U test. B, representative photographs. Scale bar, 100 µm. C, vessel stabilization was analyzed by staining of pericytes by anti–α-smooth muscle actin. Results are expressed as mean (± SEM) percentage pericyte-stabilized CD31/α-smooth muscle actin double-positive blood vessels compared with the total number of CD31-positive blood vessels. For this calculation, vessels were classified in small, medium, and large size. D, representative photographs of tumor sections stained with anti-CD31 (blue) and anti–α-smooth muscle actin (pink).

research groups showed antitumoral activity of CXCL4/PF-4[47-70] and of modified fragments of CXCL4/PF-4[47-70] at higher doses (0.25 mg/kg/d and with continuous administration using minipumps) in a glioma and glioblastoma model (20, 21, 32).

The molecular mechanism of the angiostatic and antitumoral activities of the CXCL4/PF-4 forms remains unclear. Several hypotheses have already been proposed for CXCL4/PF-4 activities. First, a newly identified receptor variant, named CXCR3-B, could act as a functional recep-

tor for CXCL4/PF-4 in mediating the inhibition of endothelial cell growth (14). Recently, Mueller et al. (33) reported that CXCL4/PF-4 at high concentration induces intracellular calcium release through CXCR3 and attracts activated T lymphocytes. However, there is no evidence for the existence of CXCR3-B in mice. In our study, we injected COOH-terminal peptides composed of 24 amino acids, lacking the NH$_2$-terminal part essential for GPCR binding, suggesting that not just CXCR3 binding is necessary for inhibition of angiogenesis. It has also been shown

that CXCL4/PF-4 binds to CXCL8/IL-8 and that they can form heterodimers (34, 35) with implications on the biological activities of CXCL4/PF-4, such as enhancement of the antiproliferative effect (35). Such heterodimers could also be involved in mediating the angiostatic activities of

CXCL4L1/PF-4var and its COOH-terminal fragment. Second, the association of chemokines and GAGs facilitates the retention of chemokines on cell surfaces and enables the formation of immobilized, or haptotactic, gradients. This is required for leukocyte recruitment by
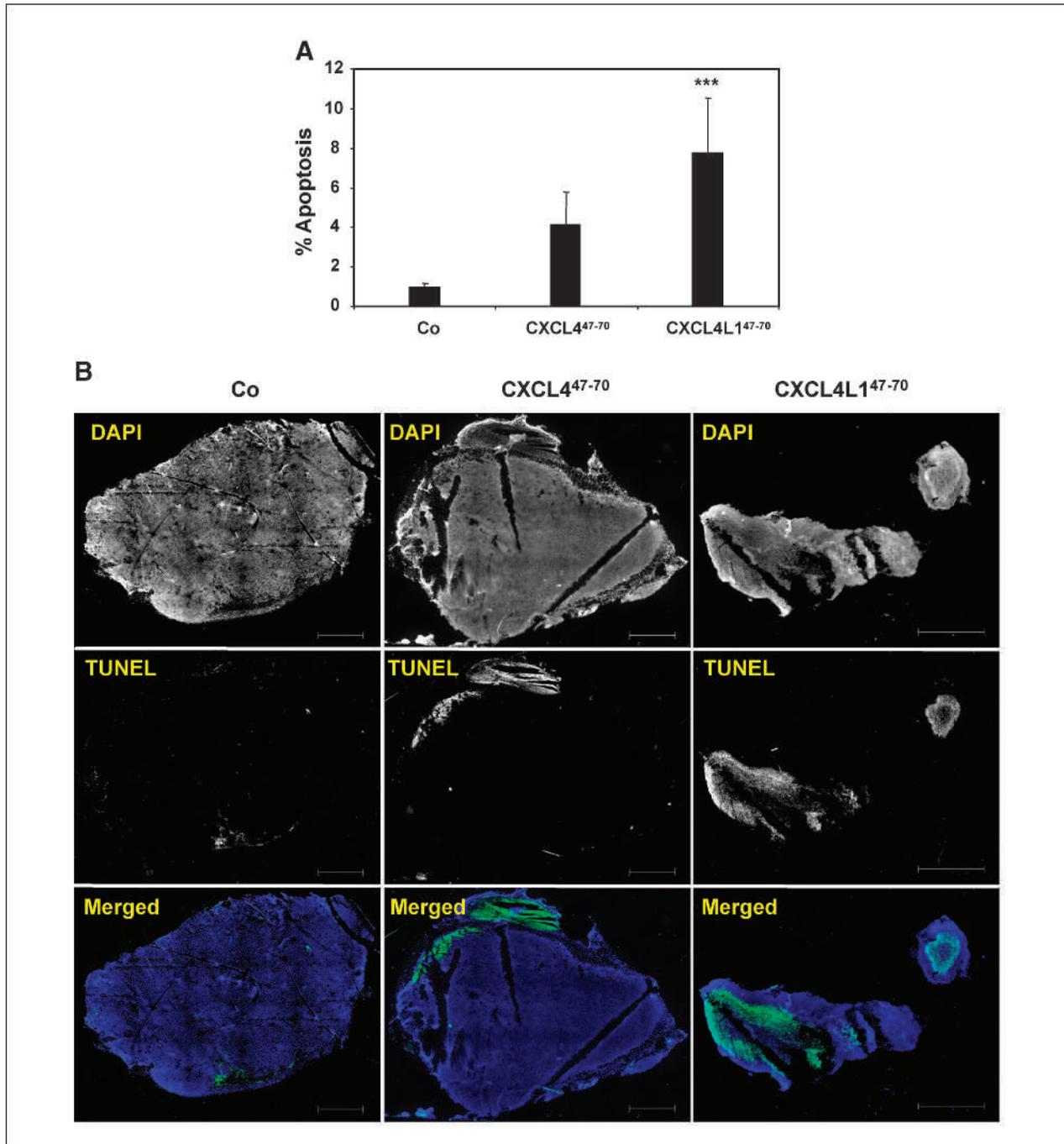
FIGURE 7. Tissue analysis of CXCL4/PF-4[47-70]–treated and CXCL4L1/PF-4var[47-70]–treated B16 melanoma for apoptosis. Tissue sections from B16 tumors treated with control solution, 1 µg CXCL4/PF-4[47-70], or 1 µg CXCL4L1/PF-4var[47-70] per injection were evaluated for apoptosis with the TUNEL assay. A, data are expressed as a percentage of the apoptotic surface area compared with the total surface area. ***, $P < 0.001$, Mann-Whitney U test. B, representative photographs. Cell nuclei were stained with DAPI (blue) and apoptotic cells were visualized in green. Scale bars, 1,000 µm.

maintaining a high local chemokine concentration (36). Moreover, chemokine-GAG interaction may facilitate the receptor binding process. In addition, GAGs are involved in many processes, such as the control of tumor cell replication, invasion, and vascularization (37). Further, on neutrophils, a chondroitin sulfate proteoglycan receptor has been identified for CXCL4/PF-4 (38), and on endothelial cells, a specific heparan sulfate binding site shared between CXCL4/PF-4 and CXCL10/IP-10 has been evidenced (39). Third, it has also been shown that CXCL4/PF-4 interferes with the angiogenic effect of FGF-2 and VEGF by disrupting the interaction of these growth factors with GAGs. CXCL4/PF-4 can also directly bind to FGF-2, preventing its dimerization, resulting in the inhibition of binding of this growth factor to its proper receptor and in the reduction of internalization of FGF-2 (40-42). In addition, CXCL4/PF-4 inhibits epidermal growth factor–stimulated proliferation of endothelial cells and interferes with the cell cycle by impaired downregulation of $p21^{CIP1/WAF1}$ (43). Further, it has been shown that different CXCL4/PF-4 peptides compete with FGF-2 or VEGF by inhibiting their binding to FGF or VEGF receptors, respectively, or reduce heparin-induced FGF-2 dimerization, resulting in the angiostatic activity (21, 31, 44, 45). However, other mechanisms seem to be involved as well because an analogue of CXCL4/PF-4 that lacks affinity for heparin still retains its angiostatic activity (46), and CXCL4/PF-4 also inhibits the function of VEGF-121, an isoform with deficient heparin-binding ability (47). Recently, an interaction of CXCL4/PF-4 with integrins has been described that might be implicated in angiogenesis (48). It should be noted that the mechanism of action of CXCL4/PF-4, the first identified member of the chemokine family, seems to be the most complex and consequently the least well understood.

In summary, this is the first report in which CXCL4L1/PF-4var[47-70] and CXCL4/PF-4[47-70], differing in only three amino acids, were compared biologically. Based on different *in vitro* and *in vivo* assays, we conclude that CXCL4L1/PF-4var[47-70] is a more potent inhibitor of angiogenesis and has a more pronounced antitumoral capacity than CXCL4/PF-4[47-70] without affecting leukocyte recruitment. In-depth studies are necessary to further clarify the molecular mechanisms through which CXCL4L1/

PF-4var[47-70] exerts its angiostatic and antitumoral activity, particularly by investigating GPCR and GAG binding, as well as growth factor interactions. Because of the small size of the peptide and its ability to inhibit many aspects of the angiogenic cascade (at relatively low doses), CXCL4L1/PF-4var[47-70] is a promising candidate as an antiangiogenic drug for cancer treatment and possibly also for other angiogenesis-dependent diseases. Indeed, identifying small active fragments of endogenous inhibitors may be useful to reduce immunogenicity and increase bioavailability. Application of engineered tumor cells or oncotropic viruses (e.g., parvovirus) to locally release chemokines, such as monocyte chemotactic protein-3 in melanoma, confirms their potential clinical value in anticancer therapy (49). In addition, administration of angiogenesis inhibitors, in combination with chemotherapy and radiation, remains an interesting approach for future cancer treatment. Several antiangiogenic compounds are currently in clinical development, as anticancer agents and some drugs, such as anti-VEGF antibodies, are already used for the treatment of cancer (50).

References

1. Deuel TF, Keim PS, Farmer M, Heinrikson RL. Amino acid sequence of human platelet factor 4. Proc Natl Acad Sci U S A 1977;74: 2256–8.
2. Luster AD. Chemokines—chemotactic cytokines that mediate inflammation. N Engl J Med 1998;338:436–45.
3. Strieter RM, Burdick MD, Mestas J, Gomperts B, Keane MP, Belperio JA. Cancer CXC chemokine networks and tumour angiogenesis. Eur J Cancer 2006;42:768–78.
4. Vandercappellen J, Van Damme J, Struyf S. The role of CXC chemokines and their receptors in cancer. Cancer Lett 2008;267:226–44.
5. Zlotnik A, Yoshie O. Chemokines: a new classification system and their role in immunity. Immunity 2000;12:121–7.
6. Murphy PM. International Union of Pharmacology. XXX. Update on chemokine receptor nomenclature. Pharmacol Rev 2002;54:227–9.
7. Rot A, von Andrian UH. Chemokines in innate and adaptive host defense: basic chemokinese grammar for immune cells. Annu Rev Immunol 2004;22:891–928.
8. Strieter RM, Kunkel SL, Elner VM, et al. Interleukin-8. A corneal factor that induces neovascularization. Am J Pathol 1992;141:1279–84.
9. Van Damme J, Van Beeumen J, Opdenakker G, Billiau A. A novel, NH₂-terminal sequence-characterized human monokine possessing neutrophil chemotactic, skin-reactive, and granulocytosis-promoting activity. J Exp Med 1988;167:1364–76.
10. Maione TE, Gray GS, Petro J, et al. Inhibition of angiogenesis by

recombinant human platelet factor-4 and related peptides. Science 1990;247:77–9.

11. Kasper B, Brandt E, Ernst M, Petersen F. Neutrophil adhesion to endothelial cells induced by platelet factor 4 requires sequential activation of Ras, Syk, and JNK MAP kinases. Blood 2006;107:1768–75.

12. Eslin DE, Zhang C, Samuels KJ, et al. Transgenic mice studies demonstrate a role for platelet factor 4 in thrombosis: dissociation between anticoagulant and antithrombotic effect of heparin. Blood 2004;104:3173–80.

13. Gewirtz AM, Zhang J, Ratajczak J, et al. Chemokine regulation of human megakaryocytopoiesis. Blood 1995;86:2559–67.

14. Lasagni L, Francalanci M, Annunziato F, et al. An alternatively spliced variant of CXCR3 mediates the inhibition of endothelial cell growth induced by IP-10, Mig, and I-TAC, and acts as functional receptor for platelet factor 4. J Exp Med 2003;197:1537–49.

15. Eisman R, Surrey S, Ramachandran B, Schwartz E, Poncz M. Structural and functional comparison of the genes for human platelet factor 4 and PF4alt. Blood 1990;76:336–44.

16. Green CJ, Charles RS, Edwards BF, Johnson PH. Identification and characterization of PF4varl, a human gene variant of platelet factor 4. Mol Cell Biol 1989;9:1445–51.

17. Struyf S, Burdick MD, Proost P, Van Damme J, Strieter RM. Platelets release CXCL4L1, a nonallelic variant of the chemokine platelet factor-4/CXCL4 and potent inhibitor of angiogenesis. Circ Res 2004;95:855–7.

18. Vandercappellen J, Noppen S, Verbeke H, et al. Stimulation of angiostatic platelet factor-4 variant (CXCL4L1/PF-4var) versus inhibition of angiogenic granulocyte chemotactic protein-2 (CXCL6/GCP-2) in normal and tumoral mesenchymal cells. J Leukoc Biol 2007;82:1519–30.

19. Struyf S, Burdick MD, Peeters E, et al. Platelet factor-4 variant chemokine CXCL4L1 inhibits melanoma and lung carcinoma growth and metastasis by preventing angiogenesis. Cancer Res 2007;67:5940–8.

20. Bello L, Giussani C, Carrabba G, et al. Suppression of malignant glioma recurrence in a newly developed animal model by endogenous inhibitors. Clin Cancer Res 2002;8:3539–48.

21. Hagedorn M, Zilberberg L, Wilting J, et al. Domain swapping in a COOH-terminal fragment of platelet factor 4 generates potent angiogenesis inhibitors. Cancer Res 2002;62:6884–90.

22. Proost P, Mortier A, Loos T, et al. Proteolytic processing of CXCL11 by CD13/aminopeptidase N impairs CXCR3 and CXCR7 binding and signaling and reduces lymphocyte and endothelial cell migration. Blood 2007;110:37–44.

23. Van Damme J, Proost P, Lenaerts JP, Opdenakker G. Structural and functional identification of two human, tumor-derived monocyte chemotactic proteins (MCP-2 and MCP-3) belonging to the chemokine family. J Exp Med 1992;176:59–65.

24. Presta M, Maier JA, Rusnati M, Ragnotti G. Basic fibroblast growth factor: production, mitogenic response, and post-receptor signal transduction in cultured normal and transformed fetal bovine aortic endothelial cells. J Cell Physiol 1989;141:517–26.

25. Strieter RM, Burdick MD, Gomperts BN, Belperio JA, Keane MP. CXC chemokines in angiogenesis. Cytokine Growth Factor Rev 2005;16:593–609.

26. Balkwill F. The significance of cancer cell expression of the chemokine receptor CXCR4. Semin Cancer Biol 2004;14:171–9.

27. Müller A, Homey B, Soto H, et al. Involvement of chemokine receptors in breast cancer metastasis. Nature 2001;410:50–6.

28. Jain RK. Molecular regulation of vessel maturation. Nat Med 2003;9:685–93.

29. Hasumi Y, Klosowska-Wardega A, Furuhashi M, Ostman A, Heldin CH, Hellberg C. Identification of a subset of pericytes that respond to combination therapy targeting PDGF and VEGF signaling. Int J Cancer 2007;121:2606–14.

30. Benny O, Kim SK, Gvili K, et al. *In vivo* fate and therapeutic efficacy of PF-4/CTF microspheres in an orthotopic human glioblastoma model. FASEB J 2008;22:488–99.

31. Hagedorn M, Zilberberg L, Lozano RM, et al. A short peptide domain of platelet factor 4 blocks angiogenic key events induced by FGF-2. FASEB J 2001;15:550–2.

32. Giussani C, Carrabba G, Pluderi M, et al. Local intracerebral delivery of endogenous inhibitors by osmotic minipumps effectively suppresses glioma growth *in vivo*. Cancer Res 2003;63:2499–505.

33. Mueller A, Meiser A, McDonagh EM, et al. CXCL4-induced migration of activated T lymphocytes is mediated by the chemokine receptor CXCR3. J Leukoc Biol 2008;83:875–82.

34. Dudek AZ, Nesmelova I, Mayo K, Verfaillie CM, Pitchford S, Slungaard A. Platelet factor 4 promotes adhesion of hematopoietic progenitor cells and binds IL-8: novel mechanisms for modulation of hematopoiesis. Blood 2003;101:4687–94.

35. Nesmelova IV, Sham Y, Dudek AZ, et al. Platelet factor 4 and interleukin-8 CXC chemokine heterodimer formation modulates function at the quaternary structural level. J Biol Chem 2005;280:4948–58.

36. Proudfoot AE, Handel TM, Johnson Z, et al. Glycosaminoglycan binding and oligomerization are essential for the *in vivo* activity of certain chemokines. Proc Natl Acad Sci U S A 2003;100:1885–90.

37. Folkman J, Shing Y. Control of angiogenesis by heparin and other sulfated polysaccharides. Adv Exp Med Biol 1992;313:355–64.

38. Petersen F, Bock L, Flad HD, Brandt E. A chondroitin sulfate proteoglycan on human neutrophils specifically binds platelet factor 4 and is involved in cell activation. J Immunol 1998;161:4347–55.

39. Luster AD, Greenberg SM, Leder P. The IP-10 chemokine binds to a specific cell surface heparan sulfate site shared with platelet factor 4 and inhibits endothelial cell proliferation. J Exp Med 1995;182:219–31.

40. Bikfalvi A. Platelet factor 4: an inhibitor of angiogenesis. Semin Thromb Hemost 2004;30:379–85.

41. Perollet C, Han ZC, Savona C, Caen JP, Bikfalvi A. Platelet factor 4 modulates fibroblast growth factor 2 (FGF-2) activity and inhibits FGF-2 dimerization. Blood 1998;91:3289–99.

42. Sulpice E, Bryckaert M, Lacour J, Contreres JO, Tobelem G. Platelet factor 4 inhibits FGF2-induced endothelial cell proliferation via the extracellular signal-regulated kinase pathway but not by the phosphatidylinositol 3-kinase pathway. Blood 2002;100:3087–94.

43. Gentilini G, Kirschbaum NE, Augustine JA, Aster RH, Visentin GP. Inhibition of human umbilical vein endothelial cell proliferation by the CXC chemokine, platelet factor 4 (PF4), is associated with impaired downregulation of p21(Cip1/WAF1). Blood 1999;93:25–33.

44. Jouan V, Canron X, Alemany M, et al. Inhibition of *in vitro* angiogenesis by platelet factor-4-derived peptides and mechanism of action. Blood 1999;94:984–93.

45. Lozano RM, Redondo-Horcajo M, Jimenez MA, et al. Solution structure and interaction with basic and acidic fibroblast growth factor of a 3-kDa human platelet factor-4 fragment with antiangiogenic activity. J Biol Chem 2001;276:35723–34.

46. Maione TE, Gray GS, Hunt AJ, Sharpe RJ. Inhibition of tumor growth in mice by an analogue of platelet factor 4 that lacks affinity for heparin and retains potent angiostatic activity. Cancer Res 1991;51:2077–83.

47. Gengrinovitch S, Greenberg SM, Cohen T, et al. Platelet factor-4 inhibits the mitogenic activity of VEGF121 and VEGF165 using several concurrent mechanisms. J Biol Chem 1995;270:15059–65.

48. Aidoudi S, Bujakowska K, Kieffer N, Bikfalvi A. The CXC-chemokine CXCL4 interacts with integrins implicated in angiogenesis. PLoS One 2008;3:e2657.

49. Wetzel K, Struyf S, Van Damme J, et al. MCP-3 (CCL7) delivered by parvovirus MVMp reduces tumorigenicity of mouse melanoma cells through activation of T lymphocytes and NK cells. Int J Cancer 2007;120:1364–71.

50. Presta LG, Chen H, O'Connor SJ, et al. Humanization of an anti-vascular endothelial growth factor monoclonal antibody for the therapy of solid tumors and other disorders. Cancer Res 1997;57:4593–9.